Original Article

Seismic performance of prefabricated composite shear wall with end steel plate connection by nonlinear finite element analysis

Yi Wang[a b *], **Chengcheng Guo**[b], **Peibo You**[a], **Hairong Wu**[a], **Zili Wang**[a], **Yansong Li**[a]

[a] School of Civil and Transportation Engineering, Henan University of Urban Construction, Pingdingshan 467036, China
[b] School of Civil Engineering and Architecture, China Three Gorges University, Yichang 443000, China
*Corresponding author: wangy213@yeah.net

Abstract

Chinese construction industry is gradually transforming to industrialization, leading to the growth of prefabricated buildings. The prefabricated steel-plate concrete composite shear wall structure has become a hotspot in architecture globally. Based on the mechanical characteristics of shear walls, an end steel plate connection prefabricated composite shear wall structure is proposed. Through numerical simulation of the prefabricated composite shear wall with different connection areas and the cast-in-place composite shear wall, the feasibility and reliability of the end steel plate connection is verified. Based on the verification, it is necessary to further study the influence of different parameters on the seismic performance of prefabricated composite shear wall with end steel plate connection. The results show that the connector length should be controlled within a reasonable range, and the tie bars in the node connection area can improve the strength and ductility of the wall. The aspect ratio and axial pressure ratio have significant influence on the seismic performance of the wall and should be reasonably selected in design.

Keywords

1. Introduction

Since the beginning of the 21st century, prefabricated building has gained popularity in China's construction industry due to its ability to industrialize the construction process and housing manufacturing. Due to its advantages in construction efficiency, economic benefits, environmental protection, and seismic capacity, it has been strongly supported by national policies. In recent years, the prefabricated composite shear wall structure has become a hotspot globally.

The node connection method plays a crucial role in ensuring the overall performance of the structure and has been extensively studied. The connection mode of prefabricated shear wall is divided into dry connection and wet connection. Research has found that the seismic performance of wet-connected prefabricated shear wall and cast-in-place shear wall is basically the same (Pan et al., 2021; Chen and Xiao, 2016; Yan et al., 2018; Tullini and Minghini, 2016). However, there are some problems in wet connection, such as difficult positioning and easy bending of extended steel reinforcements, as well as poor controllability of grouting quality, leading to wet connection gradually being replaced by dry connection. The welded connection (Wei and Li, 2020; Shen et al., 2019) and mortise-tenon connection (Sun et al., 2021; Yu et al., 2022) can meet the seismic requirements of prefabricated shear wall. However, welding connection can lead to brittle failure, affecting the bearing capacity and deformation capacity of the whole structure. The mortise-tenon connection requires high strength of cast-in-place concrete and steel reinforcements on both sides of the wall, increasing the complexity of fabrication and installation due to the irregular wall shape. Bolt connection (Li et al., 2021; Cheng et al., 2019) has the advantages of excellent seismic performance and convenient construction. However, traditional bolt connections often use embedded parts and connecting steel frames for full-section connection, which increases the construction cost and installation accuracy. To address the above problems, scholars such as Soudki et al. (1995), Zhong et al. (2022) and Lim et al. (2016), have suggested using box bolted connections at the end of pre-made shear wall nodes. Research has shown that this structure can meet seismic requirements and improves deformation and energy dissipation of shear walls. Only the end connection cannot lead to the overturning of the shear wall or the early failure in the middle part of shear walls, indicating that this connection form has reliability. However, in the box bolt connection at the end of prefabricated shear wall nodes, it is impossible to avoid the problems of high installation accuracy and narrow operating space inside the box. For this reason, the prefabricated composite shear walls connected by T-shaped plate and butt plate in the early stage are studied (Wang et al., 2023; Wang et al., 2022). The results show that the seismic
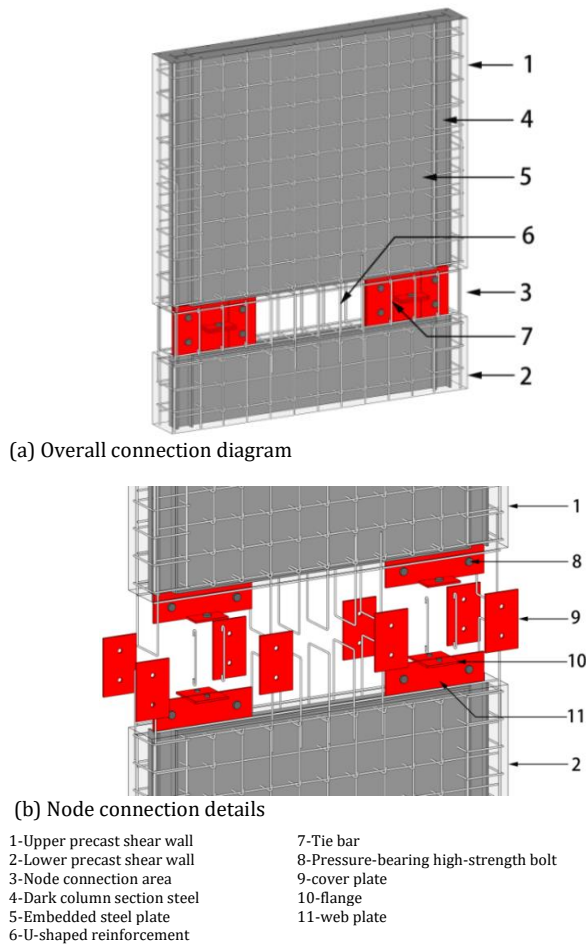
performance of the prefabricated composite shear wall connected by butt plate is better than that of the T-shaped plate connection. The T-shaped plate connection can directly connect the flanges without setting the gasket and the vertical positioning devices. Compared with the butt plate connection, it can improve the prefabrication efficiency and solve the problems of high installation precision and narrow operation surface.

Combined the T-shaped plate with the butt plate, a prefabricated composite shear wall with end steel plate connection is proposed. It can improve the prefabricated efficiency and enhance the bearing performance of the wall. At the same time, it can solve problems of easy bending of the overhanging steel bar, difficult positioning of the steel bar, large amount of steel plate bolts, high installation accuracy requirements, and narrow operation space in the joint connection area. The feasibility and reliability of this connection method are verified using the finite element software ABAQUS. Meanwhile, the influence of different parameters on the seismic performance of the wall is studied. Finally, a calculation method for the bearing capacity of the prefabricated composite shear wall is proposed, providing a theoretical basis for their application in engineering practice.

2. Test survey

2.1 Node design

The connection structure of the end steel plate connection prefabricated composite shear wall joint is shown in Fig.1. First, the flanges are directly connected, which is a pre-embedded extension connector of the upper and lower prefabricated walls. It is fixed with high-strength bolts under pressure to achieve vertical positioning and installation. Then both sides of the cover plate and the web plate are connected by pressure-bearing high-strength bolts. Second, the horizontal distribution reinforcement is set in the connection area of the node. The tie bars are set at the rigid connectors at both ends of the horizontal distribution bars, and the U-shaped bars are set at the gap of the rigid connectors. The U-shaped steel bar is embedded and extended in the upper and lower prefabricated walls. The extension section of the U-shaped steel bar is tied with the horizontal distribution reinforcement in the joint connection area. Finally, the concrete is poured to form a complete connection node.

(a) Overall connection diagram

(b) Node connection details

1-Upper precast shear wall	7-Tie bar
2-Lower precast shear wall	8-Pressure-bearing high-strength bolt
3-Node connection area	9-cover plate
4-Dark column section steel	10-flange
5-Embedded steel plate	11-web plate
6-U-shaped reinforcement	

Fig. 1 End steel plate connection structure diagram

2.2 Test piece design

The prefabricated composite shear wall with end steel plate connection is 1500mm×1000mm×120mm, with the heights of the upper and lower precast walls being 1200mm and 150mm, respectively. The post-pouring belt has a height of 150mm. The loading beam is 1200mm×200mm×200mm, with a steel I section of 70mm×35mm×10mm inside. The ground beam is 1600mm×500mm×300mm. The longitudinal reinforcement of the upper wall extends into the loading beam by 180mm, and that of the lower wall extends into the ground beam by 470mm. The dark column steel I-section is 54mm×50mm×5mm, and the built-in steel plate has a thickness of 5mm. The dark column section-steel and the built-in steel plate are extended into the loading beam by 70mm; the built-in steel plate extends into the ground beam by 300mm, and the dark column section-steel extends into the ground beam by 430mm. The specific size and reinforcement of the shear wall are shown in Fig.2. At the end of the node connection area, the bolts are made of M16 bearing high strength bolts. The stiff connector web at the end of the node extends 75mm from the upper and lower prefabricated wall, the width of the flange on both sides of the web is 92mm, and the overall steel plate thickness is 5mm. The specific size of the rigid connector at the end of the joint is shown in Fig.3.
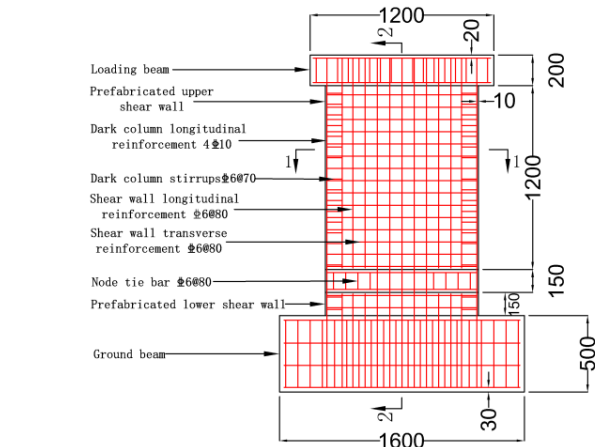
2.3 Parametric analysis scheme

First, the finite element numerical simulation is conducted on cast-in-place composite shear wall (XJ-1) and prefabricated composite shear wall (PCSW-T-1 / 2) with different node connection areas to verify the feasibility and reliability of end steel plate connection. Then, the influence of different parameters on the seismic performance of prefabricated composite shear wall with end steel plate connection is studied. The specific analysis scheme is shown in Table 1. The specific numbering rules are as follows: PCSW-X-N: PCSW represents the prefabricated composite shear wall; X is represented by T connection area, L connector length, S node tie bar, A axial pressure ratio, and D aspect ratio. N represents the same set of the test code number. XJ-1 is a cast-in-place composite shear wall.

2.4 Material mechanical

The strength and specification of concrete, steel reinforcement and steel plate in the prefabricated composite shear wall with end steel plate connection are the same as those in Ref. (Wu, 2014). The material properties are selected from the measured data in Ref. (Wu, 2014), as shown in Table 2 and Table 3. At the same time, according to the
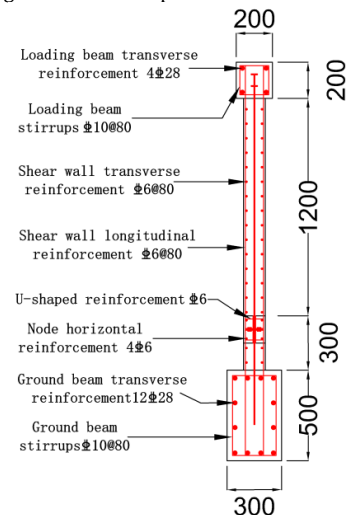
constitutive model expressions of concrete under uniaxial tension and compression recommended in the Code for Design of Concrete Structures (GB50010-2010), the constitutive relationship curve of concrete is obtained as shown in Fig.4. The bilinear model is used to define the uniaxial stress-strain curve of steel plate and steel reinforcement, as shown in Fig.5
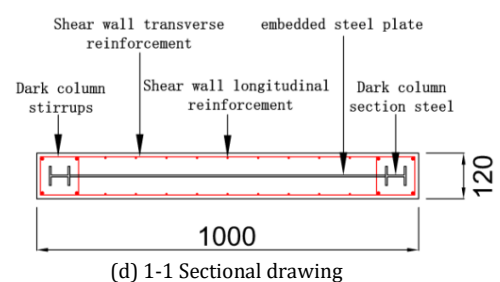

(a) Reinforcement diagram
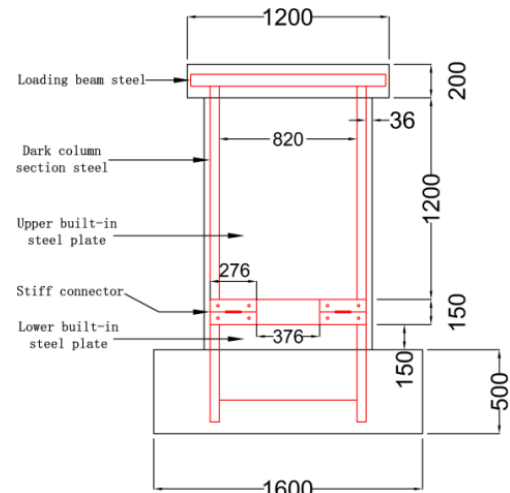
(b) Schematic diagram of the steel plate

(c) 2-2 Side view

(d) 1-1 Sectional drawing

Fig. 2 Dimensions and reinforcement

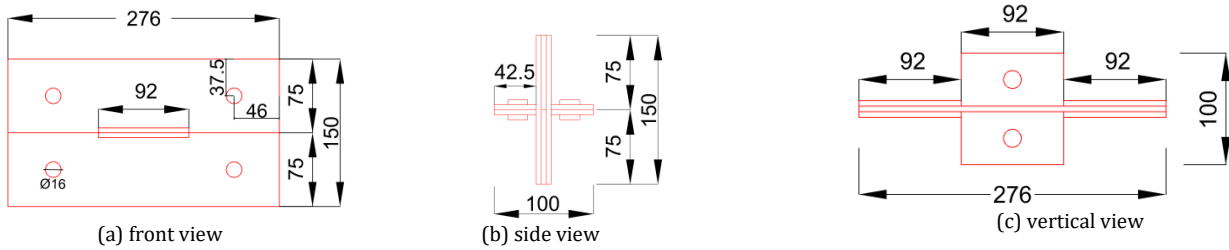(a) front view   (b) side view   (c) vertical view

Fig. 3 Three view of the end steel plate connector

Table 1. Parametric analysis

Group number	Test piece number	Node connection area	Connector length (mm)	Node tie bar	Axial pressure ratio	Aspect ratio
0	XJ-1	-	-	-	0.3	1.5
1	PCSW-T-1	Node end	276	Existence	0.3	1.5
	PCSW-T-2	Node end and middle				
2	PCSW-L-1	Node end	236	Existence	0.3	1.5
	PCSW-L-2		276			
	PCSW-L-3		316			
3	PCSW-S-1	Node end	276	Non-existence	0.3	1.5
	PCSW-S-2			Existence		
4	PCSW-A-1	Node end	276	Existence	0.3	1.5
	PCSW-A-2				0.4	
	PCSW-A-3				0.6	
5	PCSW-D-1	Node end	276	Existence	0.3	1
	PCSW-D-2					1.5
	PCSW-D-3					2

Table 2. Concrete strength value

Strength grade	cube crushing strength $f_{cu,k}$/MPa	prism compressive strength f_{ck}/MPa	axial tensile strength f_{tk}/MPa	Elastic modulus E_c/MPa
C80	76	57.76	4.13	37962

Table 3. Steel material parameters

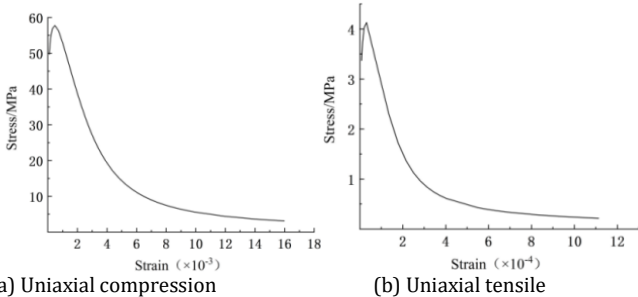| Material	Yield strength f_y/MPa	Ultimate strength f_u/MPa	Elastic modulus E_s/MPa
Steel plate	416.20	536.70	205000
Steel reinforcement	409.45	521.38	210000
Bolt	846.00	941.00	210000

(a) Uniaxial compression   (b) Uniaxial tensile
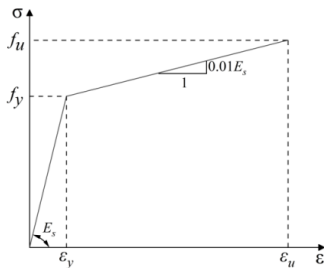
Fig. 4 Concrete constitutive relation curve

Fig. 5 Steel constitutive relation curve

3. Finite element simulation of prefabricated composite shear wall with end steel plate connection

3.1 Finite element modeling

Unit selection and grid division

The model selects the three-dimensional solid element C3D8R for concrete, steel plate and bolt. The steel reinforcement adopts three-dimensional truss element T3D2.The grid of the wall is 25mm; the grid of the built-in steel plate, section-steel and steel reinforcement is 30mm, and the grid of the loading beam and the ground beam is 80 mm. The mesh of the rigid connectors and bolts is12 mm and 6 mm respectively.

Interaction

In the finite element analysis, it is considered that there is a good binding force between concrete, steel plate and steel reinforcement. The embedded command is used to embed steel plates and steel reinforcement into concrete; binding constraints are selected for contact between concretes. The contact surfaces of rigid connectors are in face-to-face contact. The normal and tangential directions are simulated through hard contact and Coulomb friction respectively. The friction coefficient is 0.6 (ACI Committee, 2008).

Boundary conditions and loading methods

The bottom of the shear wall ground beam is completely fixed. The reference point is set at the center point of the top surface of the loading beam, so that the reference point and the top surface of the loading beam are coupled by the Coupling command. Finally, a displacement boundary condition is applied at this coupling point to limit the out-of-plane displacement of the wall.

The application of load is mainly divided into two steps. In the first step, the axial load is calculated according to the design axial compression ratio of the specimen, and the axial load is applied to the coupling point at the top of the loading beam. During the whole loading process, the axial load should be kept constant. In the second step, the horizontal reciprocating load is applied by displacement loading at the top coupling point of the loading beam, and each level of load is cycled once. It is stipulated that the load applied on the left side is positive and the load applied on the right side is negative, and the test is stopped until the specimen is destroyed or the ultimate load drops to 85 % of the peak load. The specific loading system is shown in Fig.6.
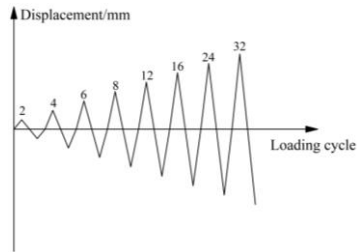
**Fig. 6 Loading system**

3.2 Finite element model verification

To verify the rationality of parameters and material constitutive calculations in the model, W1-aand W1-b (Wu, 2014) are selected for finite element numerical simulation. The dimensions of the specimen, reinforcement, and finite element model are shown in Figs.7 and 8. Numerical simulation is carried out by applying the same load as the specimen. Finally, the hysteresis curve, skeleton curve and ultimate bearing capacity are obtained as shown in Fig.9, Fig.10 and Table 4.
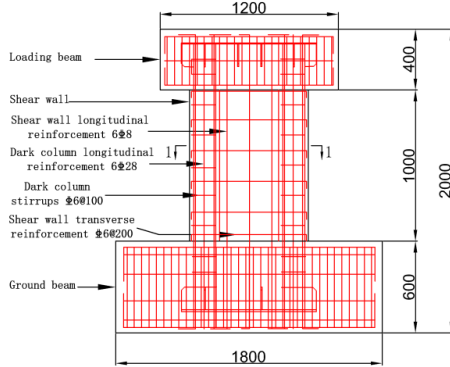
(a) Reinforcement details
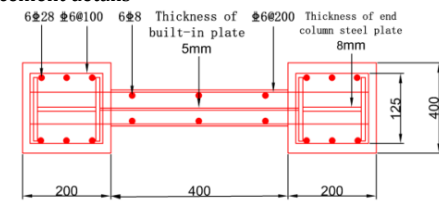
(b) W1-a Sectional drawing
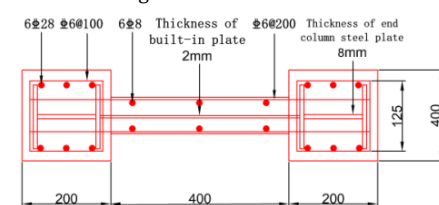
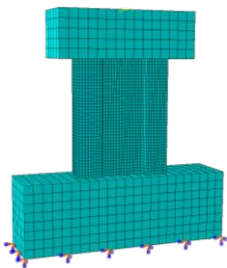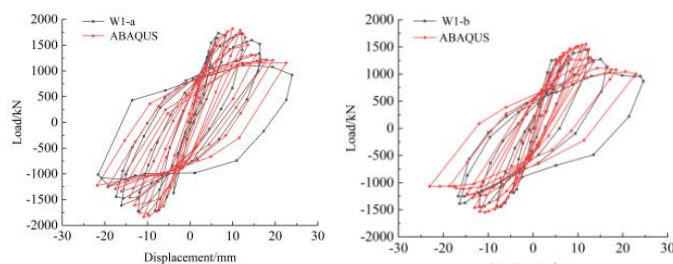(c) W1-b Sectional drawing

Fig. 7 Specimen and reinforcement details

Figu. 8 Finite element model of the specimen
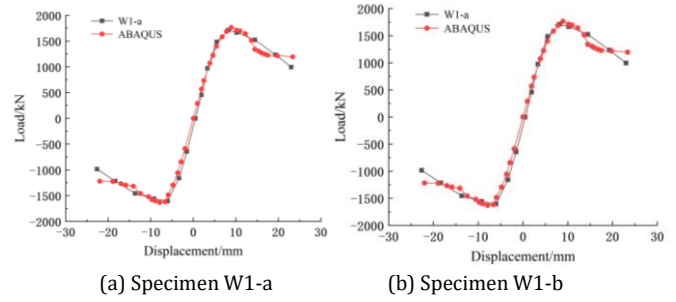

(a) Specimen W1-a   (b) Specimen W1-b

Fig. 9 Diagram of hysteresis curve comparison

It can be seen from Fig.9 that the hysteretic curves of the two specimens are basically consistent with the experimental results. However, the fullness of the hysteresis loop in the later stage of loading is significantly lower than the test results. The main reason is that the bond slip between steel reinforcement and steel plate in concrete is not considered in the finite element simulation, which reduces the energy dissipation capacity in the later stage and leads to the shrinkage of the hysteresis loop.

(a) Specimen W1-a   (b) Specimen W1-b

**Fig. 10 Diagram of skeleton curve comparison**

Table 4. Comparison of ultimate bearing capacity

Test piece number	Ultimate bearing capacity/kN		Error/%
	Experimental value	Value of simulation	
W1-a	1709.77	1763.80	3.16
W1-b	1454.94	1553.04	6.74

From Fig.10, the skeleton curves of the two are basically the same. According to the comparison of the ultimate bearing capacity in Table 4, the simulated value of the specimen is higher than the experimental value. The main reason is that the finite element simulation ignores the bond-slip of the built-in steel plate and steel reinforcement in concrete. However, based on the comparison of numerical simulation and experimental results, the error of the two results is within 10 %. It indicates that the above modeling method can effectively simulate the real test results, and the rationality and accuracy of the above modeling parameters are verified.

4. Seismic performance analysis

To study the seismic performance of the prefabricated composite shear wall with end steel plate connection, the finite element models of PCSW-T-1/2and XJ-1are established (Fig.11). There is no node connection area in XJ-1. The specific dimensions of the reinforcement are shown in Fig. 12. Using the loading method described in Section 3.1.3, the finite element numerical simulation is conducted on the models PCSW-T-1/2 and XJ-1, and the simulation results are compared and analyzed for comparison.
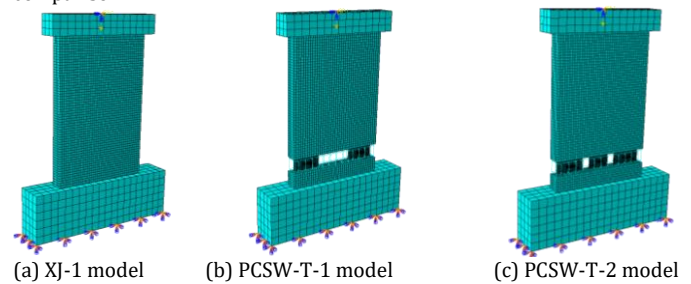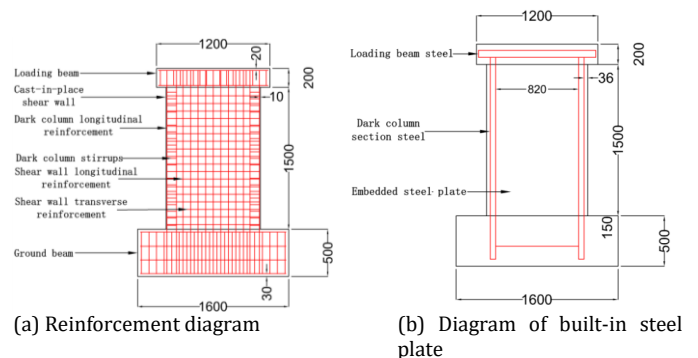

(a) XJ-1 model   (b) PCSW-T-1 model   (c) PCSW-T-2 model

Fig. 11 Finite element model of the specimens

(a) Reinforcement diagram   (b) Diagram of built-in steel plate

Fig. 12 Dimensions and reinforcement of the cast-in-place composite shear wall

4.1 Bearing capacity analysis

Fig.13 and Table 5 show the comparison of hysteresis curve, skeleton curve and bearing capacity between PCSW-T-1/2and XJ-1.
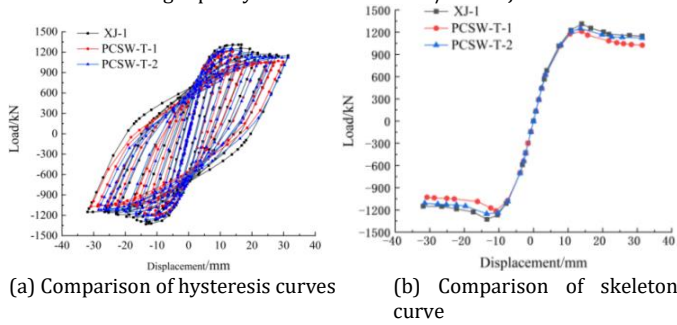

(a) Comparison of hysteresis curves

(b) Comparison of skeleton curve

Fig. 13 Comparison of specimen curves

From Fig. 13 (a), the hysteresis curves of the three specimens are spindle shaped. The results show that the seismic performance and energy dissipation capacity of PCSW-T-1/2 are basically the same as that of XJ-1. From Fig. 13(b), the skeleton curves of the three are basically consistent before reaching the peak load. The PCSW-T-1 curve is lower than XJ-1 and PCSW-T-1 curves after peak load. It shows that the end steel plate connection has little effect on the bearing capacity of the prefabricated composite shear wall.

Table 5. Comparison of bearing capacities

Number	Yield load f_y/kN	Peak load f_u/kN
XJ-1	1137.42	1320.09
PCSW-T-1	1068.01	1212.29
PCSW-T-2	1095.50	1251.65

According to Table 5, the ultimate bearing capacity of specimen PCSW-T-1 is 107.8, 39.36kN different from test piece XJ-1 and PCSW-2, respectively. The main reason is that the PCSW-T-1 connector is only connected at the end of the node, and the vertical load in the middle of the wall is transmitted through the U-shaped reinforcement, without using steel plate or rigid connector. Therefore, the bearing capacity is reduced. Since the error value is within 10 %, it meets the requirements of seismic performance.

4.2 Strength analysis

Under the action of reciprocating load, the strength of the specimen will decrease as the cycles increase. The strength will degrade rapidly due to the increasing cumulative damage, and the overall seismic performance of the structure will be directly affected. Therefore, strength degradation can be used as one of the important parameters to evaluate the seismic performance of the structure. The overall load degradation coefficient λ_j represents the overall strength degradation characteristics of the structure (Pang, 2017). The strength degradation of precast composite shear walls and cast-in-place composite shear walls is shown in Fig.14. λ_j is calculated as follows:

$$\lambda_j = \frac{P_j}{P_{max}} \quad (1)$$

where P_j is the peak load corresponding to the j-level loading displacement, and Pmax is the extreme point load of the skeleton curve.
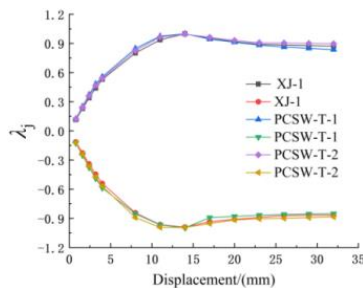

Fig. 14 Comparison of strength degradation curves of the specimens

Fig.14 shows the strength degradation of the overall load of the specimens. The strength degradation curves of the three changes basically the same. When the horizontal displacement reaches 14 mm, the peak strength point is obtained. The later strength degradation rate is basically consistent. It shows that only the steel plate connection at the end of the node has no significant effect on the strength degradation of the prefabricated composite shear wall.

4.3 Ductility analysis

Ductility refers to the deformation ability of a structure from yield to ultimate failure. It is an important parameter index to study the seismic performance of structures, and usually described quantitatively by the ductility coefficient μ (Miranda and Bertero, 1994).

$$\mu = \frac{\Delta_u}{\Delta_y} \quad (2)$$

where Δ_u is the ultimate displacement, and Δ_y is the yield displacement. Here the drawing method is used to determine the yield displacement (Fig.15). The ultimate displacement is the corresponding displacement point when the bearing capacity decreases to 85% of the peak load; If not, the maximum displacement point corresponding to the last loading is taken. According to the above method, the ductility factors of PCSW-T-1/2 and XJ-1 are shown in Table 6.
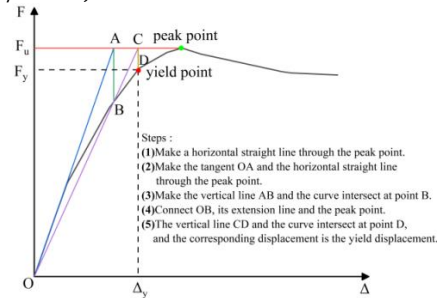

Fig. 15 Diagram of the drawing method

Table 6. Comparison of ductility coefficients

Numbering	Δ_y/mm	Δ_u/mm	μ
XJ-1	9.37	31.44	3.36
PCSW-T-1	8.71	31.46	3.61
PCSW-T-2	8.80	31.43	3.57

Table 6 shows that the ductility coefficients of PCSW-T-1 / 2 specimens are basically the same. The ductility coefficient of specimen XJ-1 decreased by about 0.23. It shows that only the end steel plate connection can improve the ductility of the precast composite shear wall.

The prefabricated composite shear wall with end steel plate connection can fully meet the requirements of seismic performance, with optimal feasibility. The influence of different parameters on its seismic performance should be further studied, providing a reference for later engineering application.

5. Simulation parameter analysis

To fully understand the seismic performance of prefabricated composite shear wall with end steel plate connection, numerical simulation and comparative analysis are carried out for each group of specimens under different parameters.

5.1 Hysteresis curve analysis

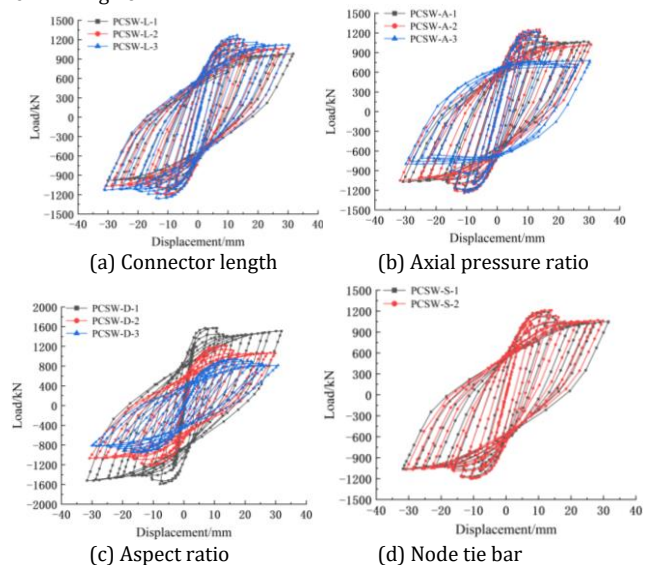Under low cyclic loading, the hysteretic behavior of each specimen is shown in Fig.16.

(a) Connector length

(b) Axial pressure ratio

(c) Aspect ratio

(d) Node tie bar

Fig. 16 Comparison of hysteretic curves of each specimen

Through Fig.16 (a), it is found that the hysteresis curves of the three are basically consistent, and only separation occurs in the later stage of loading. It shows that the increase of the length of the connector has no significant effect on the hysteretic performance of the shear wall, which only causes the decrease of the peak load.

Through Fig.16 (b), it is found that the hysteretic curve of the specimen SPCW-A-3 is fuller in the later stage of loading, but it is lower than the model SPCW-A-1/2. This shows that the increase of axial compression ratio will cause the bearing capacity of shear wall to decrease, but the wall is mainly loaded by steel plate after failure, and the overall hysteretic performance is obviously improved.

Through Fig.16 (c), it is found that the pinching degree of the hysteresis curves of the three increases with the increase of the aspect ratio. It shows that the increase of height-width ratio will lead to a significant decrease in hysteresis performance.

Through Fig.16 (d), it is found that the hysteresis curves of the two are basically consistent, indicating that the existence of the tie bar has no effect on the hysteresis performance of the shear wall.

5.2   Bearing capacity analysis

Based on the finite element numerical simulations, the comparison of the skeleton curves of each group of specimens is shown in Fig.17.
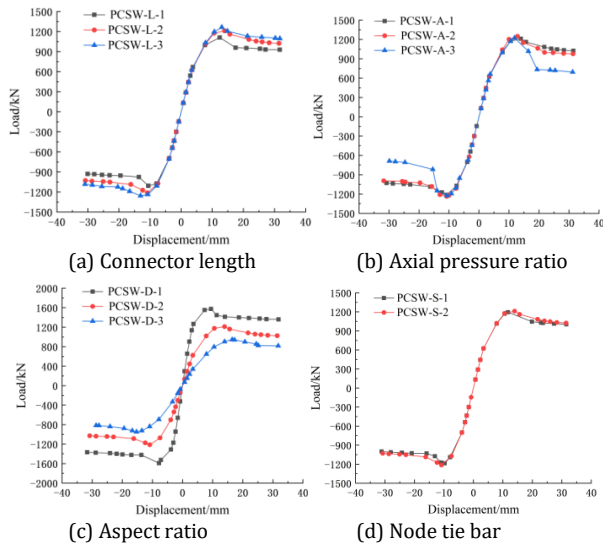

(a) Connector length   (b) Axial pressure ratio

(c) Aspect ratio   (d) Node tie bar

Fig. 17 Comparison of skeleton curves of each specimen

From Fig.17 (a), the skeleton curves of PCSW-L-1 / 2 specimens are basically the same and higher than those of PCSW-L-3 specimens. Increasing the connector after reaching a certain length has no significant effect on the bearing capacity. The main reason is that both sides of the shear wall are mainly subjected to tension and compression and shear force under reciprocating load. When the connector is short, the tensile performance of the steel decreases, leading to the bearing capacity of the specimen decreasing. The middle part of the shear wall is only subjected to a certain range of compression and shear, mainly borne by concrete. The increase in the connector length does not contribute much to the compressive performance. Hence it is feasible to connect the steel plate only at the end of the prefabricated composite shear wall.

From Fig.17 (b), the skeleton curve of the specimen PCSW-A-1/2 is always in an agreement. However, the skeleton curve of the specimen PCSW-A-3 decreases significantly after reaching the peak load, indicating that large axial pressure ratio will lead to a sudden decrease in the bearing capacity of the wall.

From Fig.17 (c), the curve is significantly separated as the aspect ratio increases, indicating that increasing the aspect ratio will significantly reduce the bearing capacity of the wall.

From Fig.17 (d), the skeleton curves of the two are basically the same, indicating that there is no significant influence on the bearing capacity of the wall through setting the tie bar in the node connection area.

5.3   Stiffness degradation analysis

The secant stiffness K is used to analyze the stiffness degradation. The stiffness degradation curves of each specimen under different parameters are obtained, as shown in Fig.18. K is calculated as follows:

$$K_i = \frac{|F_i| + |-F_i|}{|\Delta_i| + |-\Delta_i|}$$

(3)

where $\pm F_i$ is the peak load of the ith positive and negative loading, and $\pm \Delta_i$ is the displacement corresponding to the peak point of the ith positive and negative loading.
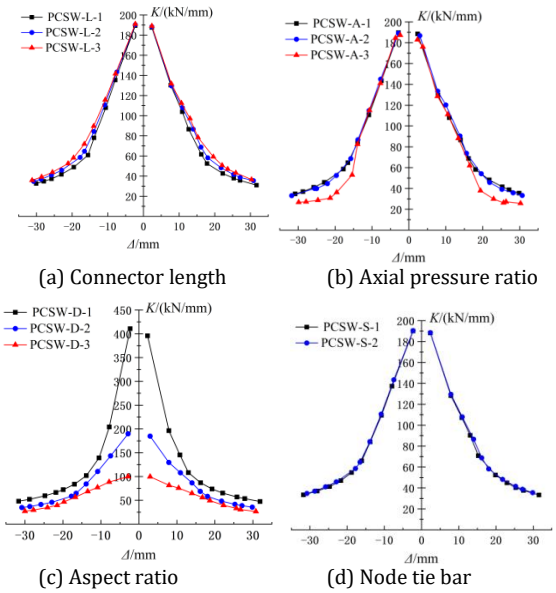

(a) Connector length   (b) Axial pressure ratio

(c) Aspect ratio   (d) Node tie bar

Fig. 18 Comparison of stiffness degradation curves of each specimen

It can be seen from Fig.18 (a) that there is no significant separation between the stiffness degradation curves of the three. It indicates that increasing the connector length has little effect on the overall lateral stiffness of the shear wall.

It can be seen from Fig.18 (b) that the initial stiffness of the three stiffness curves is basically the same, due to the large axial compression ratio of the specimen PCSW-A-3. The stiffness degradation rate of the specimen is accelerated in the later stage of loading. It indicates that when the axial compression ratio is too large, the stiffness degradation rate of the shear wall is faster in the later stage of loading.

It can be seen from Fig.18 (c) that the stiffness curves of the three are obviously separated in the early stage of loading, and gradually tend to coincide in the later stage of loading. It indicates that as the aspect ratio increases, the initial stiffness of the shear wall will decrease significantly. The stiffness degradation rate tends to be gentle, with optimal overall lateral stiffness.

It can be seen from Fig.18 (d) that the stiffness degradation curves of the two are in good agreement. It indicates that the tie bars in the node connection area have no significant effect on the overall lateral stiffness of the wall.

5.4   Strength degradation analysis

The strength degradation curve of each specimen under different parameters is shown in Fig.19. ZX and FX represent the positive loading and negative loading, respectively.

(a) Connector length   (b) Axial pressure ratio

(c) Aspect ratio   (d) Node tie bar
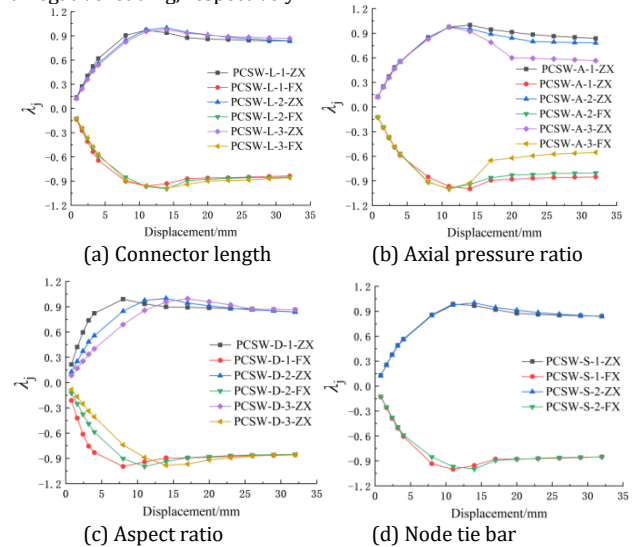
Fig. 19 Comparison of strength degradation curves of each specimen

Fig.19 (a) shows that the strength degradation point of PCSW-L-1 is earlier than PCSW-L-2/3. It indicates that as the connector length increases, the strength degradation of the wall will be delayed; when the connector length exceeds a certain range, it has no significant effect on the overall strength of the shear wall.

Fig.19 (b) shows that the separation is gradually significant as the axial pressure ratio increases in the later stage of loading. The strength degradation curve of the low axial pressure ratio PCSW-A-1/2 is more gently than that of the high axial pressure ratio PCSW-A-3 after reaching the peak load. It shows that excessive axial pressure ratio will lead to rapid decline of the later strength of shear wall.

Fig.19 (c) shows that as the aspect ratio increases, the strength degradation curves of the three are significantly separated in the initial stage of loading, and the late loading tends to coincide. The intensity peak points move backward in sequence. As the aspect ratio increases, the strength of the shear wall increases, and the degradation rate tends to plateau.

Fig.19 (d) shows that the strength degradation curves of the two are basically the same. The peak strength point of PCSW-S-2 is delayed than that of PCSW-S-1. It is explained that setting tie bars at node connections can avoid early strength degradation of shear walls.

5.5 Ductility analysis

Based on the results of the finite element simulation analysis, the yield displacement and ultimate displacement of each specimen are determined according to the method described in Section 4.3. Finally, the ductility coefficient of each specimen is shown in Table 7.

Table 7. Comparison of ductility coefficients

Group number	Numbering	Δ_y/mm	Δ_u/mm	μ
1	PCSW-L-1	7.71	24.52	3.18
	PCSW-L-2	8.71	31.46	3.61
	PCSW-L-3	8.84	31.73	3.59
2	PCSW-S-1	8.59	26.77	3.12
	PCSW-S-2	8.71	31.46	3.61
3	PCSW-A-1	8.71	31.46	3.61
	PCSW-A-2	8.88	31.43	3.54
	PCSW-A-3	8.97	19.96	2.22
4	PCSW-D-1	6.98	31.52	4.52
	PCSW-D-2	8.71	31.46	3.61
	PCSW-D-3	12.16	31.80	2.62

From Table 7, when the connector length exceeds a certain range, it has no significant effect on the overall ductility of the shear wall. The tie bars at the node can improve the ductility of the shear wall. As the axial pressure ratio and aspect ratio increase, the ductility of shear wall will decrease.

6. Theoretical analysis of bearing capacity

The calculation method for bearing capacity in the early stage (Wang et al., 2023) is adopted. Consideration: The gap between the connecting parts can still be regarded as a steel plate opening. The reduction of steel plate thickness can be used to replace the influence of steel plate opening. That is, based on the calculation method of bearing capacity of cast-in-place composite shear wall in the current code (Ministry of Housing and Urban-Rural Development of the People's Republic of China, 2016), the bearing capacity of steel plate is reduced, and the calculation formula for bearing capacity of assembled composite shear wall is obtained as follows:

$$(4)$$

$$V = \frac{1}{\lambda - 0.5}\left(0.5 f_t b_w h_{w0} + 0.13 N \frac{A_w}{A}\right) + f_{yh}\frac{A_{sh}}{s}h_{w0} + \frac{0.3}{\lambda}f_a A_{a1} + \frac{0.6}{\lambda - 0.5}f_p A_p'$$

where is the cross-sectional area of the steel plate after thickness reduction, (Wang et al.,2023). The remaining symbolic meanings are shown in (Ministry of Housing and Urban-Rural Development of the People's Republic of China, 2016).

To verify the reliability of the calculation method of bearing capacity, the theoretical calculation of the specimen under different parameters is carried out according to Formula (4). The results are shown in Table 8.

Table 8. Comparison of analytical and theoretical values

Numbering	Analysis value/kN	Theoretical value/kN	Error magnitude/%
PCSW-T-1	1212.29	1278.87	5.49
PCSW-T-2	1251.65	1278.87	2.17
PCSW-L-1	1109.21	1158.55	4.45
PCSW-L-2	1212.29	1278.87	5.49
PCSW-L-3	1260.83	1407.16	11.61
PCSW-A-1	1212.29	1278.87	5.49
PCSW-A-2	1242.81	1278.87	2.90
PCSW-A-3	1224.35	1278.87	4.45
PCSW-D-1	1582.47	1752.06	10.72
PCSW-D-2	1212.29	1278.87	5.49
PCSW-D-3	946.81	945.01	-0.19

It can be seen from Table 8 that the error between the theoretical value and the analytical value is about 10%, which is optimal. It shows that this calculation method has certain feasibility and applicability.

7. Conclusion

A prefabricated composite shear wall structure with end steel plate connection is proposed, and its seismic performance is verified through variable parameter analysis. Finally, the theoretical analysis of bearing capacity is carried out. The following main conclusions are drawn:

1. The bearing capacity and strength of the prefabricated composite shear wall with end steel plate connection are basically the same as those of the cast-in-place composite shear wall, and its ductility performance is better than that of the cast-in-place composite shear wall. There is no significant difference in bearing capacity, strength, and ductility between the prefabricated composite shear wall with end steel plate connection and the prefabricated composite shear wall with both end and middle connections.
2. When the connector length in the node connection area exceeds a certain range, the overall performance of the shear wall is not significantly improved. To reduce the construction cost, it is recommended to reduce the connector length between 200mm and 300mm.
3. The tie bars in the joint connection area can improve the strength and ductility of the shear wall. However, it has no obvious effect on the hysteretic performance, bearing capacity and stiffness degradation.
4. The aspect ratio and axial pressure ratio have a significant effect on the seismic performance index of the prefabricated composite shear wall with end steel plate connection. It should be controlled within a reasonable range in the design. An axial pressure ratio of 0.3 -0.5, and an aspect ratio of 1.5-1.8 are suggested.
5. The finite element analysis results of prefabricated composite shear wall with end steel plate connection are basically consistent with the calculation results of the bearing capacity. The feasibility and effectiveness of the finite element analysis are demonstrated. The applicability of the original bearing capacity calculation method is further verified.

The prefabricated composite shear wall with endplate connection can fully meet the requirements of seismic performance. However, the effects of different bolt diameters, slip between connectors and concrete, and openings of shear walls on the seismic performance of prefabricated composite shear walls with end steel plate connections should be further considered. Our future work would focus on the experiments on the prefabricated composite shear wall with end steel plate connection.

Acknowledgements

References

ACI Committee. (2008). Building code requirements for structure concrete (ACI318-08) and commentary[S]. American Concrete Institute.

Chen, J., Xiao, Y. (2016). Experimental study on seismic behavior of precast concrete columns with longitudinal reinforcement grouting-anchoring connections. China Civil Engineering Journal, vol.49, no.05, pp.63-73. https://Doi: 10.15951/j.tmgcxb.2016.05.006

Cheng, B., Zhang, Q., Li, W.F. (2019). Research on mechanical properties of connection for a new prefabricated reinforced concrete shear wall. Industrial Construction, vol.49, no.2, pp. 49-54+65. https://Doi:10.13204/j. gyjz201902011

Feng, P., Qiang, H.L., Ye, L.P. (2017). Discussion and definition on yeid points of materials members and structures. Engineering Mechanics, vol.34, no.3, pp.36-46. https://Doi:10.6052/i.issn.1000-4750.2016.03.0192

Li, W., Gao, H., Xiang, R., & Du, Y. (2021). Experimental study of seismic performance of precast shear wall with a new bolt-plate connection joint. Structures, vol.34, pp.3818-3833. https://Doi: 10.1016/j.istruc.2021.10.009

Lim, W. Y., Kang, T. H. K., & Hong, S. G. (2016). Cyclic lateral testing of precast concrete t-walls in fast low-rise construction. ACI Structural Journal, vol.113, no.1, pp.179-189. https://Doi:10.14359/51688200

Ministry of Housing and Urban-Rural Development of the People's Republic of China. (2016). Code for design of composite structures JGJ 138-2016 [S]. Beijing: China Building Industry Press.

Miranda, E., & Bertero, V. V. (1994). Evaluation of strength reduction factors for earthquake-resistant design. Earthquake Spectra, vol.10, no.2, pp.357-379. https://Doi:10.1193/1.1585778

Pan, G.B., Cai, J., Yang, C., Xu, M.Z., Chen, Q.J., Zhu, D.F., Chen, Q.R., Zuo, Z.L. (2021). Experimental study on seismic behavior of precast RC shear walls connected by extruding steel sleeves and rebars. Journal of Building Structures, vol.42, no.5, pp.111-120. https://Doi:10.14006/j.jzjgxb.2020.C034

Pang, Y. (2017). Seismic behavior tests and numerical analyses of composite shear walls with double steel plates and infill concrete. Hefei University of Technology.

Shen, S. D., Pan, P., Miao, Q. S., Li, W. F., & Gong, R. H. (2019). Test and analysis of reinforced concrete (RC) precast shear wall assembled using steel shear key (SSK). Earthquake Engineering & Structural Dynamics, vol.48, no.14, pp.1595-1612. https://Doi:10.1002/eqe.3215

Soudki, K. A., Rizkalla, S. H., & LeBlanc, B. (1995). Horizontal connections for precast concrete shear walls subjected to cyclic deformations part 1: mild steel connections. PCI Journal, vol.40, no.4, pp.78-96. https://Doi:10.15554/PCIJ.07011995.78.96

Sun, Z.J., Cao, C.L., Liu, J.L., Li, X.B., Chen, G.Y., Chu, M.J. (2021). Experimental study on mechanical behaviors of assembled monolithic shear walls with mortise-tenon joints under different shear span ratio. Building Structure, vol.51, no.9, pp.23-29. https://Doi:10.19701/j.jzjg.2021.09.004

Tullini, N., & Minghini, F. (2016). Grouted sleeve connections used in precast reinforced concrete construction - Experimental investigation of a column -to- column joint. Engineering Structures, vol.127, pp.784-803. https://Doi: 10.1016/j.engstruct.2016.09.021

Wang, Y., Wang, Z., You, P., Zhao, J., &Hao, X. (2022). Seismic Performance Assessment of Bolt Connection-based Assembled Composite Shear-wall. Iranian Journal of Science and Technology, Transactions of Civil Engineering, vol.46, no.5, pp.3723-3737. https://Doi:10.1007/s40996-021-00816-3

Wang, Y., You, P.B., Qu, S.Z., Zhang, C.Y., Zhao, J. (2023). Study on seismic properties of prefabricated composite shear walls with T-plate connections. Building Structure, vol.53, no.2, pp.92-99. https://Doi: 10.19701/j.jzjg.ls210357

Wei, H., Li, Q.N. (2020). Experimental study on seismic behavior of prefabricated RC shear walls with horizontal joints welded by steel plates. Journal of Building Structures, vol.41, no.9, pp.77-87. https://Doi: 10.14006/j.jzjgxb.2019.0541

Wu, X.C. (2014). Study on seismic behavior of composite shear wall with high strength concrete and infill steel plates. South China University of Technology.

Yan, Q., Chen, T., & Xie, Z. (2018). Seismic experimental study on a precast concrete beam-column connection with grout sleeves. Engineering Structures, vol.155, pp.330-344. https://Doi: 10.1016/j.engstruct.2017.09.027

Yu, X.X., Chu, M.J., Li, X.B., Liu, J.L. (2022). Finite element simulation of mechanical behavior of monolithic precast shear wall with concrete tenon and mortise under medium and high shear span ratio. Building Structure, vol.52, no. S1, pp. 1794-1800. https://DOI: 10.19701/j.jzjg.22S1120

Zhong, X., Chen, Z.X., Jiang, Q., Huang, J.Q., LI, H.R., Fang, X.W., Xie, J.C. (2022). Research on seismic performance of prefabricated concrete shear wall structures with bolt connections. Industrial Construction, vol.52, no.11, pp.12-18+90. https://Doi:10.13204/j. gyjzG21012705